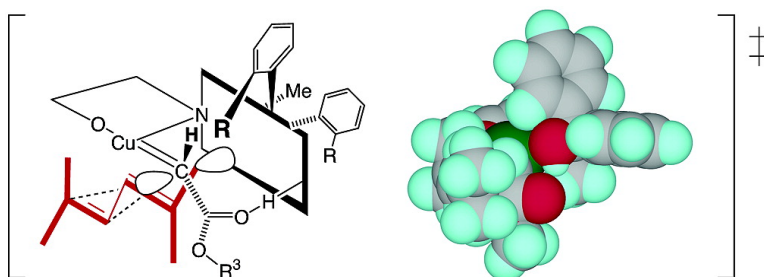


Reaction Pathway and Stereoselectivity of Asymmetric Synthesis of Chrysanthemate with the Aratani C-Symmetric Salicylaldimine–Copper Catalyst

Katsuhiro Suenobu, Makoto Itagaki, and Eiichi Nakamura

J. Am. Chem. Soc., **2004**, 126 (23), 7271-7280 • DOI: 10.1021/ja031524c • Publication Date (Web): 21 May 2004

Downloaded from <http://pubs.acs.org> on March 31, 2009



More About This Article

Additional resources and features associated with this article are available within the HTML version:

- Supporting Information
- Links to the 4 articles that cite this article, as of the time of this article download
- Access to high resolution figures
- Links to articles and content related to this article
- Copyright permission to reproduce figures and/or text from this article

[View the Full Text HTML](#)

Reaction Pathway and Stereoselectivity of Asymmetric Synthesis of Chrysanthemate with the Aratani C_1 -Symmetric Salicylaldimine–Copper Catalyst

Katsuhiro Suenobu,* Makoto Itagaki, and Eiichi Nakamura*

Contribution from the Organic Synthesis Research Laboratory, Sumitomo Chemical Co., Ltd., 1-98, Kasugade-naka, 3-chome, Konohana-ku, Osaka 554-8558, Japan, and Department of Chemistry, The University of Tokyo, Bunkyo-ku, Tokyo 113-0033, Japan

Received December 4, 2003; E-mail: suenobu@sc.sumitomo-chem.co.jp; nakamura@chem.s.u-tokyo.ac.jp

Abstract: The reaction pathway and the mechanism of asymmetric induction in the synthesis of (+)-*trans*-(1*R*,3*R*)-chrysanthemate methyl ester from methyl diazoacetate and 2,5-dimethyl-2,4-hexadiene in the presence of a C_1 -chiral salicylaldimine Cu(I) complex has been probed with the aid of hybrid density functional calculations. The key finding is that the alkoxy carbonyl carbene complex intermediate is intrinsically chiral and that the intramolecular hydrogen bonding in the carbene complex transmits the chirality information from the side chain to the carbene complex. Molecular orbital backgrounds of the structure of the carbene complex and the transition state of the cyclopropanation have been elucidated.

I. Introduction

Copper-catalyzed asymmetric cyclopropanation of an olefin with a diazo compound is a reaction of historical and practical importance.^{1–3} The Nozaki/Noyori discovery in 1966 that ethyl diazoacetate reacts with styrene in the presence of a copper catalyst bearing an optically active salicylaldimine ligand to give optically active ethyl 2-phenylcyclopropanecarboxylate recorded the first example of homogeneous catalysis with a soluble chiral metal complex.^{1–4} After numerous experimental trials and errors on both the improvement of the chiral salicylaldimine ligand and the manipulation of potentially hazardous diazo compounds, Aratani et al. at Sumitomo Chemical Co. raised the overall efficiency of the process to an industrially feasible level (Scheme 1) and achieved enantioselective syntheses of chrysanthemate acid esters, alkyl 2,2-dimethyl-3-(2-methylpropenyl)cyclopropanecarboxylate,^{1–3,5,6} and permethrinic acid esters, alkyl 3-(2,2-dichlorovinyl)-2,2-dimethylcyclopropanecarboxylate.^{2,3,6,7} Chrysanthemate and permethrinic esters represent the acid part of the structure of the most important class of insecticide, pyrethroid insecticides.^{6,8} An important practical merit of the Aratani

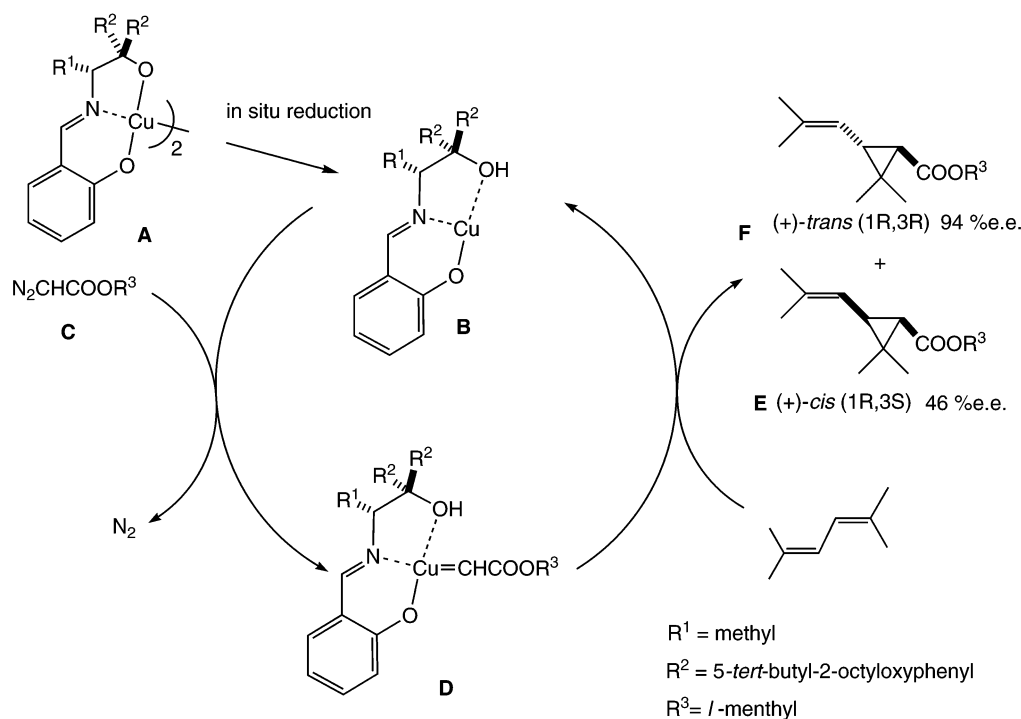
experimental protocol is that the copper catalyst is supplied as a stable Cu(II) complex, which is reduced in situ into a catalytically active Cu(I) species with an added reducing agent or with the diazo reactant.⁹ In the mid-1980s, the Aratani asymmetric process was brought into a large-scale industrial production of (*S*)-2,2-dimethylcyclopropanecarboxylic acid,^{1–3,6} a crucial part of the structure of an in vivo stabilizer of the antibiotic imipenem.^{2,6} This achievement represents the third large-scale industrial use of transition metal-catalyzed asymmetric synthesis after two earlier examples (asymmetric hydrogenation and hydrogen migration)¹⁰ and provided the first example of an asymmetric C–C bond formation process in industry. While there is an enormous current interest in C_2 -symmetric chiral ligands, C_1 systems such as the Aratani catalyst are no less important in practice. On the other hand, the mechanisms of asymmetric induction with the C_1 chiral ligands are less obvious than the (seemingly simple) mechanisms of C_2 ligands. On the basis of our previous studies on Simmons-Smith cyclopropanation¹¹ and rhodium-catalyzed carbene reactions,¹² we will decipher in the present article the factors that are responsible for the success of the Aratani system and give an overall picture of asymmetric cyclopropanation by this historically and practically important catalyst.

The mechanism of the metal-catalyzed cyclopropanation reaction of a diazo compound has been studied extensively by experiments and recently by theory,^{13,14} and the consensus is

- (1) Lebel, H.; Marcoux, J.; Molinaro, C.; Charette, A. B. *Chem. Rev.* **2003**, *103*, 977–1050.
- (2) (a) Doyle, M. P. In *Catalytic Asymmetric Synthesis*; Ojima, I., Ed.; VCH Publishers: New York, 1993. (b) Doyle, M. P. In *Catalytic Asymmetric Synthesis*, 2nd ed.; Ojima, I., Ed.; Wiley-VCH: New York, 2000.
- (3) Doyle, M. P.; McKervey, M. A.; Ye, T. *Modern Catalytic Methods for Organic Synthesis with Diazo Compounds*; John Wiley & Sons: New York, 1998.
- (4) (a) Nozaki, H.; Moriuti, S.; Takaya, H.; Noyori, R. *Tetrahedron Lett.* **1966**, 5239–5244. (b) Nozaki, H.; Takaya, H.; Moriuti, S.; Noyori, R. *Tetrahedron* **1968**, 3655–3669.
- (5) (a) Aratani, T.; Yoneyoshi, Y.; Nagase, T. *Tetrahedron Lett.* **1975**, 1707–1710. (b) Aratani, T.; Yoneyoshi, Y.; Nagase, T. *Tetrahedron Lett.* **1977**, 2599–2602.
- (6) Aratani, T. *Pure Appl. Chem.* **1985**, *57*, 1839–1844.
- (7) Aratani, T.; Yoneyoshi, Y.; Nagase, T. *Tetrahedron Lett.* **1982**, *23*, 685–688.
- (8) Arlt, D.; Jautelat, M.; Lantzsch, R. *Angew. Chem., Int. Ed. Engl.* **1981**, *20*, 703–722.

- (9) Kosower, E. M. *Acc. Chem. Res.* **1971**, *4*, 193–198.
- (10) The Monsanto asymmetric hydrogenation (*L*-DOPA synthesis) and the Takasago asymmetric hydrogen transfer (*l*-menthol synthesis).
- (11) Nakamura, M.; Hirai, A.; Nakamura, E. *J. Am. Chem. Soc.* **2003**, *125*, 2341–2350.
- (12) (a) Nakamura, E.; Yoshikai, N.; Yamanaka, M. *J. Am. Chem. Soc.* **2002**, *124*, 7181–7192. (b) Yoshikai, N.; Nakamura, E. *Adv. Synth. Catal.* **2003**, *345*, 1159–1171.
- (13) Fraile, J. M.; Garcia, J. I.; Martínez-Merino, V.; Mayoral, J. A.; Salvatella, L. *J. Am. Chem. Soc.* **2001**, *123*, 7616–7625.

Scheme 1



that the copper-catalyzed cyclopropanation reaction proceeds in two steps, carbene complex formation and carbene transfer, as discussed by Aratani for the synthesis of an alkyl chrysanthemate (Scheme 1).^{1–3,6} First, the stable Cu(II) precatalyst **A** is reduced in situ to an active catalytic Cu(I) species **B**. The structure of **A** shown as a dimer is due to X-ray crystallographic analysis,¹⁵ and that of **B** is based on analogy to this crystal structure. Then, an alkyl diazo ester **C** reacts with **B** to give a copper(I)–carbene complex **D**, the structure of which is shown here as suggested by Aratani. While there is a recent report on NMR detection of a copper(I)–carbene complex in such a reaction,¹⁶ there has been no proof of the Aratani structure **D** (for which we propose a new structure in this article). The process of a carbene complex formation from a diazo compound was detailed previously for rhodium carbenoid formation.¹² The reaction of the carbene complex with an olefin then produces a cyclopropane product and regenerates the catalyst **B**. In the reaction with 2,5-dimethyl-2,4-hexadiene (DMHD), there are two stereochemical problems, diastereoisomerism (cis and trans isomers, **E** and **F**), and enantioisomerism.

Extensive experimental studies in this laboratory have shown that the substituents R^1 – R^3 on the ligand and the ester group affect both the diastereo- and the enantioselectivity. The R^2 group is typically a 2-substituted phenyl group (crucial to achieve high stereoselectivity), which may also have a 5-substituent (least important). The R^1 and R^3 groups may be any organic groups. For one of the best combinations, $R^1 = \text{Me}$, $R^2 = 5\text{-}tert\text{-butyl-2-octyloxyphenyl}$, and $R^3 = l\text{-menthyl}$, the trans/cis ratio is 93:7, and the trans isomer is 94% ee and the cis

isomer is 46% ee (Scheme 1).^{1,3,5,6} The enantioselectivity decreases as the R^1 group becomes bulkier in the order methyl, benzyl, isopropyl, and isobutyl. In contrast, it increases as the 2-substituent in the R^2 phenyl group becomes bulkier (suggesting a far-reaching steric effect); for instance, 5-*tert*-butyl-2-octyloxyphenyl group is the best choice (however, the *tert*-butyl group is irrelevant to the stereoselectivity).⁶ As the R^3 group in the diazo ester **C** become bulkier (e.g., a *tert*-butyl group), both the diastereo- and the enantioselectivity increase.^{5b,6} There is a recent report on beneficial effects of a *p*-nitro group on the salicylalidimine moiety,¹⁷ which we ascribe to the longer lifetime of the active chiral catalyst rather than the intrinsic selectivity of the ligand.^{17d} To the best of our knowledge, there has been no model that systematically accounts for the experimental data.

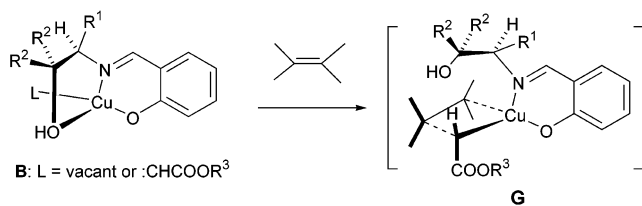
Of the four isomers of chrysanthemic acid, (+)-(1*R*,3*R*)-trans and (+)-(1*R*,3*S*)-cis isomers show insecticidal activity.⁶ From the practical point of view, the lower trans/cis selectivity is acceptable since the cis isomer can be isomerized into the trans isomer without loss of enantiomeric purity. High overall enantioselectivity, low cost, and overall high chemical efficiency are the primary goals of the chrysanthemic acid synthesis. In this respect, recently reported chiral ligands such as semicorrins,¹⁸ bis(oxazolines),¹⁹ and bipyridines²⁰ have yet to be competitive with the Aratani catalyst.

(14) (a) Bühl, M.; Terstegen, F.; Löffler, F.; Meynhardt, B.; Kierse, S.; Müller, M.; Näther, C.; Lüning, U. *Eur. J. Org. Chem.* **2001**, 2151–2160. (b) Rasmussen, T.; Jensen, J. F.; Østergaard, N.; Tanner, D.; Ziegler, T.; Norrby, P. *Chem. Eur. J.* **2002**, *8*, 177–184. (c) Straub, B. F.; Gruber, I.; Rominger, F.; Hofmann, P. *J. Organomet. Chem.* **2003**, *684*, 124–143.
 (15) (a) Yanagi, K.; Minobe, M. *Acta Crystallogr.* **1987**, *C43*, 1045–1048. (b) Yanagi, K.; Minobe, M. *Acta Crystallogr.* **1987**, *C43*, 2060–2063.
 (16) Straub, B. F.; Hofmann, P. *Angew. Chem., Int. Ed.* **2001**, *40*, 1288–1290.

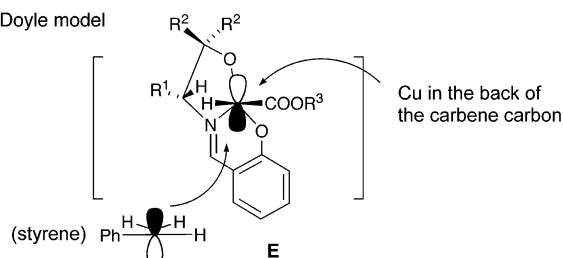
(17) (a) Li, Z.; Zheng, Z.; Chen, H. *Tetrahedron: Asymmetry* **2000**, *11*, 1157–1163. (b) Li, Z.; Liu, G.; Zheng, Z.; Chen, H. *Tetrahedron* **2000**, *56*, 7187–7191. (c) Li, Z.; Zheng, Z.; Wan, B.; Chen, H. *J. Mol. Catal. A: Chem.* **2001**, *165*, 67–71. (d) Itagaki, M.; Hagiya, K.; Kamitamari, M.; Masumoto, K.; Yamamoto, Y. Unpublished experimental results.
 (18) (a) Fritschi, H.; Leutenegger, U.; Pfaltz, A. *Helv. Chim. Acta* **1988**, *71*, 1553–1565. (b) Pfaltz, A. *Acc. Chem. Res.* **1993**, *26*, 339–345.
 (19) (a) Evans, D. A.; Woerpel, K. A.; Hinman, M. M.; Faul, M. M. *J. Am. Chem. Soc.* **1991**, *113*, 726–728. (b) Evans, D. A.; Woerpel, K. A.; Scott, M. J. *Angew. Chem., Int. Ed. Engl.* **1992**, *31*, 430–432. (c) Lowenthal, R. E.; Masamune, S. *Tetrahedron Lett.* **1991**, *32*, 7373–7376.
 (20) (a) Ito, K.; Katsuki, T. *Tetrahedron Lett.* **1993**, *34*, 2661–2664. (b) Ito, K.; Katsuki, T. *Synlett* **1993**, 638–640.

Scheme 2

(a) Aratani model



(b) Doyle model



In this article we will describe the theoretical study on the synthesis of (+)-(1*R*,3*R*)-*trans*-chrysanthemic acid methyl ester by the cyclopropanation of DMHD with methyl diazoacetate in the presence of the Aratani catalyst.

II. Chemical Models and Computational Methods

Chemical Models. For 30 years since the initial discovery, the mechanism of asymmetric induction of the Aratani catalysis has been discussed to reach no consensus: For instance, two different models have been advanced by Aratani and by Doyle; these are shown in Scheme 2.

The Aratani model (Scheme 2a)⁶ assumes the active catalysis as the copper(I) complex **B** where the copper atom is tetrahedrally coordinated by the three intramolecular ligand atoms. The carbene ligand occupies the site L, and then Aratani considered that the cycloaddition takes place via a metallacyclobutane intermediate **G**, where the stereoselectivity is determined. The stereochemical influence of the imine side chain appears rather obscure in this model, and a recent theoretical study indicates that the cyclopropane reaction least likely takes place via such a metallacyclobutane intermediate.¹³

In Doyle's model, illustrated for the reaction with styrene (Scheme 2b),^{2a,3,21} the carbene complex retains all three ligand heteroatoms, and the carbene moiety protrudes (toward the viewer) from the plane including the three heteroatoms. Styrene approaches the carbene center in such a manner that the interaction of the phenyl group on styrene with the two bulky aryl groups is minimized. On the basis of the above models (which were eventually abandoned in the present study), we studied the reaction of methyl diazoacetate with DMHD, giving (+)-*trans*-(1*R*,3*R*)-methyl chrysanthemate in two stages for the chemical models shown in Figure 1. The salicyaldimine model **I** was used for calculation of the overall reaction profile.

Models **IIa** and **IIb** that lack the benzene ring were employed to study the enantioselectivity. Model **IIa** is an achiral model where R¹ and R² are hydrogen atoms, and the latter is a chiral model [(*R*)-configuration] where R¹ and R² are methyl and phenyl groups, respectively. The achiral model **IIa** was used to find stable conformers of the Cu(I)–carbene complex. The chiral

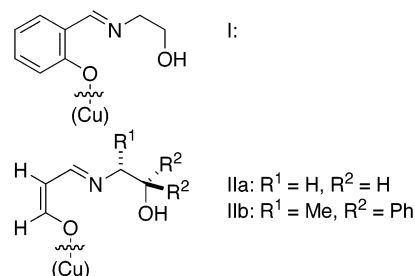


Figure 1. Models of ligands for the Cu(I) center.

model **IIb** was used to probe the enantioselection in the transition states of the reaction with DMHD, forming (+)- and (–)-*trans* methyl chrysanthemates.

Computational Methods. Geometry optimizations of all stable structures and transition states reported here were performed with the B3LYP hybrid density functional method²² implemented in a Gaussian 98 program.²³ For salicyaldimine models **I** and **IIa**, the 6-31G(d) basis set²⁴ was used for all atoms. For model **IIb** bearing a stereogenic center and two phenyl groups, the 3-21G basis set²⁵ was used for R¹ (= methyl), R² (= phenyl), and the ester methyl group, and the 6-31G(d) set was used for the remaining atoms [denoted as 6-31G(d)+3-21G]. The 6-31G(d) basis set was used by Fraile et al.¹³ for their study on copper-catalyzed cycloaddition. All the atomic charges described in this article were calculated with the natural population analysis at the B3LYP/6-31G(d) level.²⁶ The calculations reported in Figure S4 in Supporting Information were carried out at the B3LYP/6-311+G(d,p)//B3LYP/6-31G(d)+3-21G level.

Normal coordinate analysis confirmed that all stationary points discussed in this article are either stable structures or transition states. The stationary points shown in Figure 2 are connected with each other on the potential surface as confirmed by intrinsic reaction coordinate analysis (IRC).²⁷ The electronic

- (22) (a) Becke, A. D. *J. Chem. Phys.* **1993**, *98*, 5648–5652. (b) Lee, C.; Yang, W.; Parr, R. G. *Phys. Rev. B* **1988**, *37*, 785–789.
- (23) (a) Frisch, M. J.; Trucks, G. W.; Schlegel, H. B.; Scuseria, G. E.; Robb, M. A.; Cheeseman, J. R.; Zakrzewski, V. G.; Montgomery, J. A., Jr.; Stratmann, R. E.; Burant, J. C.; Dapprich, S.; Millam, J. M.; Daniels, A. D.; Kudin, K. N.; Strain, M. C.; Farkas, O.; Tomasi, J.; Barone, V.; Cossi, M.; Cammi, R.; Mennucci, B.; Pomelli, C.; Adamo, C.; Clifford, S.; Ochterski, J.; Petersson, G. A.; Ayala, P. Y.; Cui, Q.; Morokuma, K.; Malick, D. K.; Rabuck, A. D.; Raghavachari, K.; Foresman, J. B.; Cioslowski, J.; Ortiz, J. V.; Baboul, A. G.; Stefanov, B. B.; Liu, G.; Liashenko, A.; Piskorz, P.; Komaromi, I.; Gomperts, R.; Martin, R. L.; Fox, D. J.; Keith, T.; Al-Laham, M. A.; Peng, C. Y.; Nanayakkara, A.; Gonzalez, C.; Challacombe, M.; Gill, P. M. W.; Johnson, B. G.; Chen, W.; Wong, M. W.; Andres, J. L.; Head-Gordon, M.; Replogle, E. S.; Pople, J. A. *Gaussian 98 (Revision A.9)*; Gaussian, Inc.: Pittsburgh, PA, 1998. (b) Frisch, M. J.; Trucks, G. W.; Schlegel, H. B.; Scuseria, G. E.; Robb, M. A.; Cheeseman, J. R.; Zakrzewski, V. G.; Montgomery, J. A., Jr.; Stratmann, R. E.; Burant, J. C.; Dapprich, S.; Millam, J. M.; Daniels, A. D.; Kudin, K. N.; Strain, M. C.; Farkas, O.; Tomasi, J.; Barone, V.; Cossi, M.; Cammi, R.; Mennucci, B.; Pomelli, C.; Adamo, C.; Clifford, S.; Ochterski, J.; Petersson, G. A.; Ayala, P. Y.; Cui, Q.; Morokuma, K.; Rega, N.; Salvador, P.; Dannenberg, J. J. K.; Malick, D. K.; Rabuck, A. D.; Raghavachari, K.; Foresman, J. B.; Cioslowski, J.; Ortiz, J. V.; Baboul, A. G.; Stefanov, B. B.; Liu, G.; Liashenko, A.; Piskorz, P.; Komaromi, I.; Gomperts, R.; Martin, R. L.; Fox, D. J.; Keith, T.; Al-Laham, M. A.; Peng, C. Y.; Nanayakkara, A.; Challacombe, M.; Gill, P. M. W.; Johnson, B.; Chen, W.; Wong, M. W.; Andres, J. L.; Head-Gordon, M.; Replogle, E. S.; Pople, J. A. *Gaussian 98 (Revision A.11)*; Gaussian, Inc.: Pittsburgh, PA, 2001.
- (24) (a) Ditchfield, R.; Hehre, W. J.; Pople, J. A. *J. Chem. Phys.* **1971**, *54*, 724–728. (b) Hehre, W. J.; Ditchfield, R.; Pople, J. A. *J. Chem. Phys.* **1972**, *56*, 2257–2261. (c) Hariharan, P. C.; Pople, J. A. *Theor. Chim. Acta* **1973**, *28*, 213–222.
- (25) Binkley, J. S.; Pople, J. A.; Hehre, W. J. *J. Am. Chem. Soc.* **1980**, *102*, 939–947.
- (26) Glendening, E. D.; Reed, A. E.; Carpenter, J. E.; Weinhold, F. NBO version 3.1.
- (27) Fukui, K. *Acc. Chem. Res.* **1981**, *14*, 363–368.

(21) Doyle, M. P. *Recl. Trav. Chim. Pays-Bas* **1991**, *110*, 305–316.

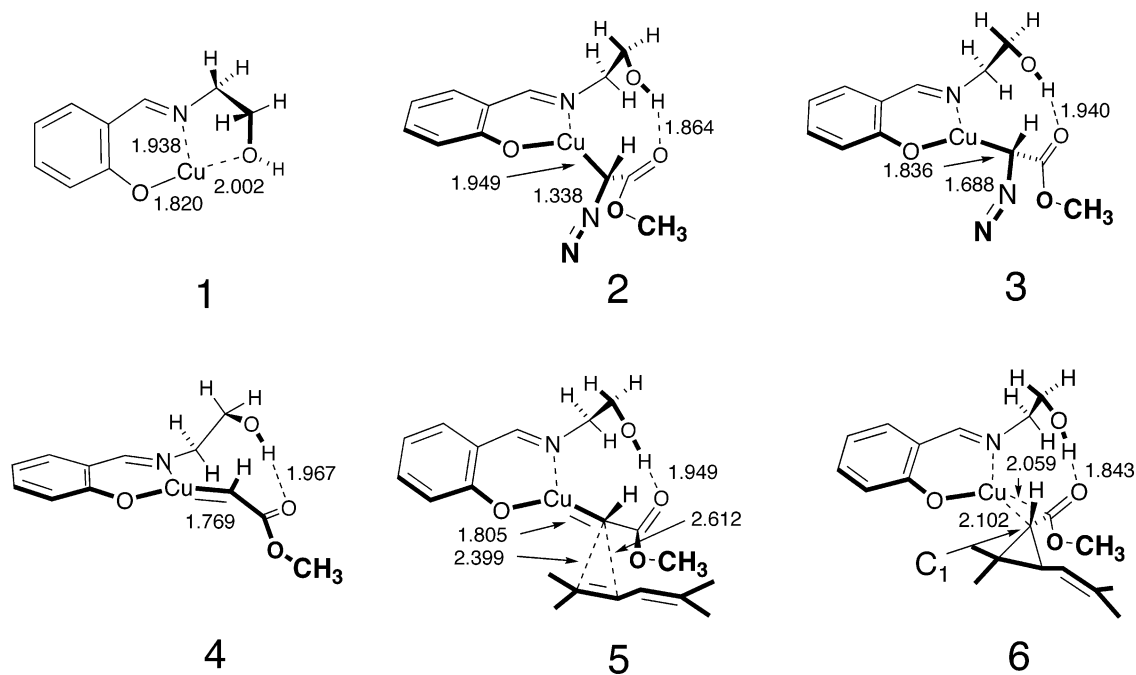


Figure 2. Optimized structures of the stationary points in the reaction profile for **I** at the B3LYP/6-31G(d) level. The number next to a bond is the interatomic distance in angstroms.

energies were corrected by non-scaled zero-point energies, and the Gibbs free energies were calculated at 298 K by the use of the frequencies without scaling. The effect of solvent polarity was considered for the overall reaction profile by use of model **I**²⁸ and found not to affect the results very much (see Figure S1 in Supporting Information). This agrees with the experimental fact that the enantio- and diastereoselectivity as well as the reaction rate is not much affected by the solvent so far as an ethereal, ester, or alkyl halide solvent is used.

III. Results and Discussion

We first studied the overall reaction profile for the achiral model ligand **I** and found that the orientation of the carbene moiety relative to the salicylaldehyde is controlled both by orbital factors and by intramolecular hydrogen bonding. Second, we searched for stable conformations of the hydrogen-bonded copper(I)–carbene complex by use of the smaller model **IIa**. Finally, we examined the transition states of the carbene insertion for the chiral model **IIb**, and the calculated selectivity was found to agree reasonably well with the experimental selectivity. Most notably, the structures of the intermediate and transition state (TS) obtained in the present study were found to have the least resemblance either to the Aratani model **D** and **G** or to the Doyle model **E**. Attempts to obtain the tetracoordinated Aratani-type structure **B** instead gave the structures discussed below (e.g., **4** in Figure 2).

A. Reaction Profile for Models I. Figure 2 shows optimized geometries of the stable structures and transition states found on a reaction pathway from the catalyst **1** bearing the ligand **I** to the product **6** (confirmed by IRC analysis). Figure 3 shows the free energy diagram at 298 K for this reaction.

In the first step toward the cyclopropane product **6**, the Cu(I) catalyst **1** and methyl diazoacetate form an α -cuprioester

complex **2**. In this step, the hydroxyl oxygen ligand in **1** is displaced by the diazoacetate to form **2** that has a Cu–C covalent bond. The hydroxy group is now hydrogen-bonded (1.864 Å) to the ester carbonyl group, the most basic atom available nearby. Back-donation of the 3d_{xz} electrons of the Cu(I) atom to the carbene center expels the molecular nitrogen via the TS **3** to form the carbene complex **4**. During this process, the Cu–C bond shrinks expectedly from 1.949 Å in **2**, to 1.836 Å in **3**, and finally to 1.769 Å in the carbene complex **4**. The molecular orbital background of these initial steps was found to be the same as the one we reported recently for a Rh-catalyzed CH activation reaction (data not shown).¹²

What is most important (cf. Conclusion section) is that the alkoxy carbene complex is intrinsically chiral. Thus, in the carbene complex **4**, the plane of the sp² carbene carbon center lies orthogonal to the plane of the salicylaldehyde and hence the carbene complex is chiral (Scheme 3). The oxygen and the nitrogen ligands donate electrons to the 3d_{xz} orbital of the copper(I) atom, which then interacts with the vacant 2p_x orbital of the carbene carbon atom. In this formalism, the copper is in its trivalent state. This scheme also illustrates the α -metallo carbonyl character of the carbene complex, as is seen in the conjugation between the C_{carbene}–Cu bond and the carbonyl π -orbital (see Figure S3 in Supporting Information).²⁹ When the imine side chain bears a stereogenic center, the orientation of the ester carbonyl group relative to the stereogenic center in the TS **5** determines the absolute stereochemistry of the C₁ carbon atom in the cyclopropane product **6**.

The cyclopropane formation takes place through the TS **5** to form the product **6**. The most notable feature (serendipitously) built into this TS is that the approach of the diene to the carbene carbon atom is limited to only one enantioface, the face opposite the imine side chain (Scheme 3). In addition, the orientation of

(28) The IPCM (isodensity surface polarized continuum model) method in Gaussian98 was used. Foresman, J. B.; Keith, T. A.; Wiberg, K. B.; Snoonian, J.; Frisch, M. J. *J. Phys. Chem.* **1996**, *100*, 16098–16104.

(29) The second-order perturbation theory analysis in the NBO analysis showed a conjugation between the Cu–C_{carbene} σ -orbital and C=O π^* -orbital (data not shown).

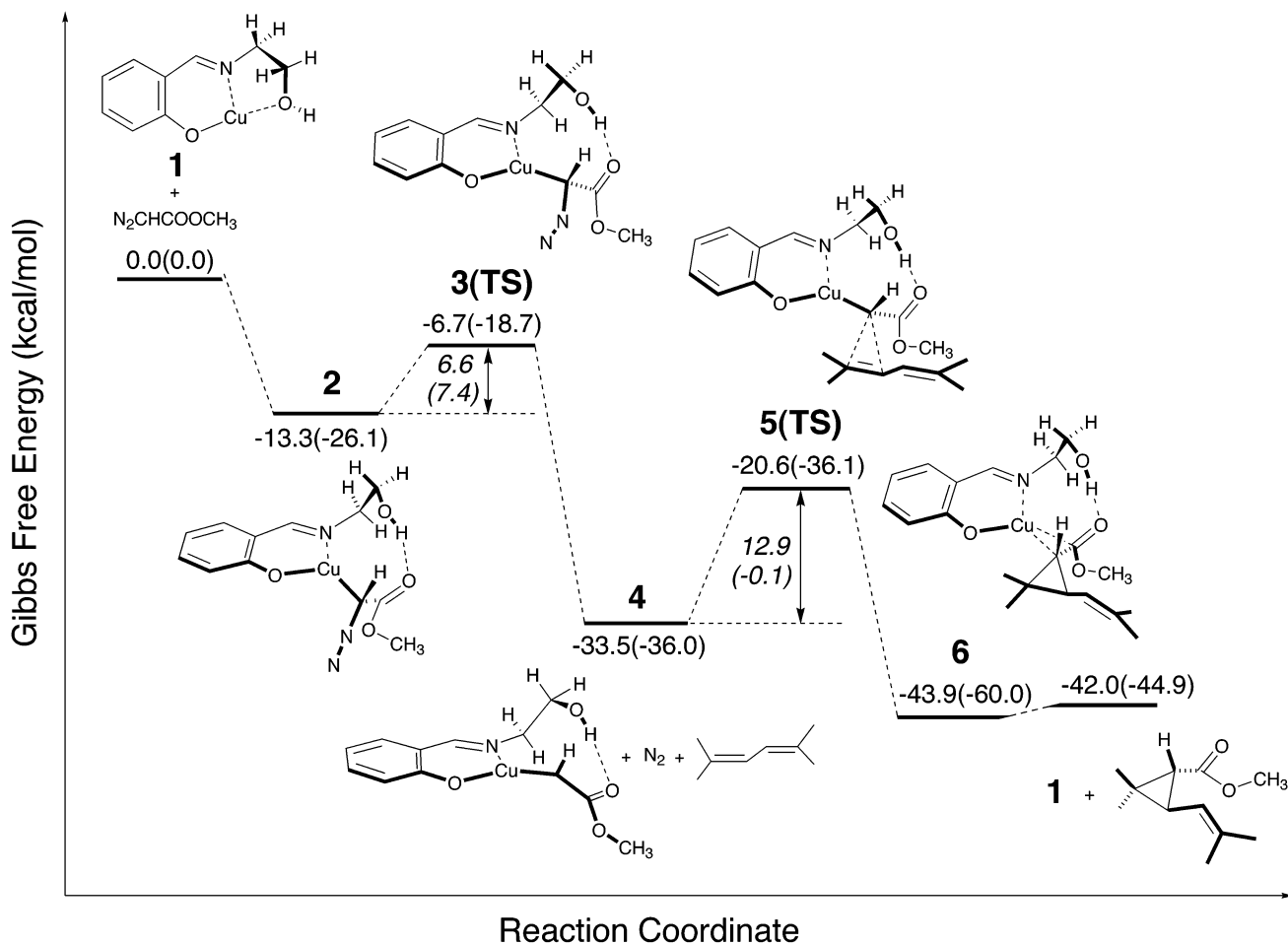
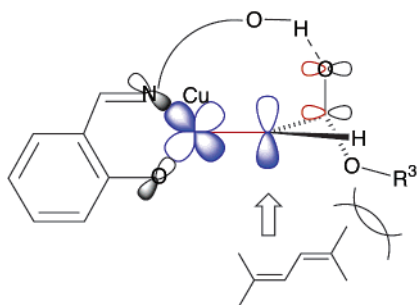


Figure 3. Gibbs free energy diagram (at 298 K in kilocalories per mole) of the reaction profile for **I** at the B3LYP/6-31G(d) level. In parentheses are relative electronic energies in kilocalories per mole. Italics indicate the free energy of activation (activation energies in parentheses).

Scheme 3. Orbital Interactions That Fix the Orientation of the Carbene Center and the Carbonyl Group^a



^a Back-donation is shown in blue, and conjugation between the Cu–C_{carbene} σ -bond and carbonyl π -orbital is shown in red. See Figure S3 in Supporting Information for the molecular orbital interaction corresponding to the α -metallo ester character.

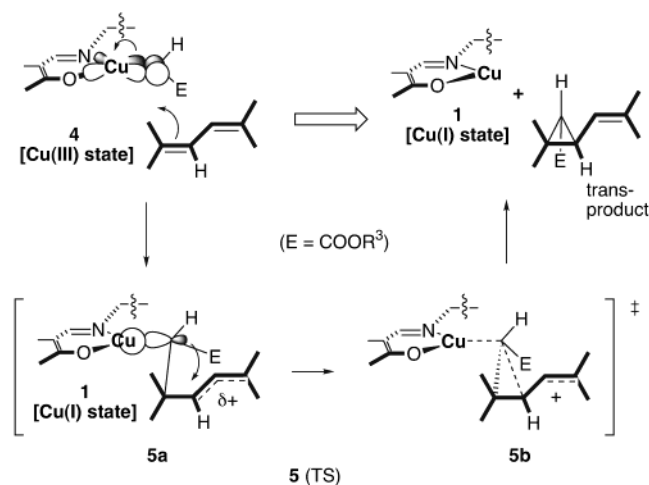
DMHD is limited to the one shown in Scheme 3. We could also locate the TSs for (–)-*trans*- and (–)-*cis*-chrysanthemates in an alternative conformation where the Me₂C=CH moiety is closer to the salicylaldimine ligand.³⁰ However, the free energies of activation for both TSs were found to be 5.5 kcal/mol higher than that for the (+)-*trans* isomer (12.9 kcal/mol). This is because that these two groups suffer severe steric hindrance owing to the propensity of the diene to maintain its planarity. Thus, these TSs are negligible in the consideration of the stereoselection mechanism.

This TS **5** of cyclopropane formation is rather early: The Cu–C bond is stretched in the TS only to the extent of 2.0%, and the C–C bond formation is not much advanced either. Note that in the C–H bond insertion reaction of the Rh–carbene complex the TS is more advanced.¹² The Rh–C_{carbene} bond is stretched as much as by 4% in the TS of the C–C bond formation. In this interaction of the carbene complex with the electron-rich diene, significant charge transfer from the diene to the carbon carbon occurs in the TS **5** (the DHMD moiety has a positive charge of +0.20), and the copper atom in the TS **5** is less positively charged by 0.05 than that in the carbene complex (+1.22). In accordance with this charge transfer, the back-donative interaction between the Cu atom and the carbene carbon is weakened, which is seen in the longer Cu–C bond (1.805 Å) in **5** than in **4** (1.769 Å).

The C–C bond formation in TS **5** is significantly asynchronous: The distance (2.399 Å) between the carbene carbon atom and the methyl-bearing diene carbon atom is much shorter than that (2.612 Å) between the carbene atom and the internal carbon atom. The Me₂C=CH moiety in the DHMD molecule is positively charged (+0.14). As in the Simmons-Smith reaction,¹¹ the olefin acts as a nucleophile toward the electron-deficient carbene carbon atom. We can therefore schematize this bond alternation process as shown in Scheme 4.

(30) The Cartesian coordinates of optimized geometries and electronic energies for the TSs of (–)-*trans*- and (–)-*cis*-chrysanthemates are described as S-5 and S-6, respectively in Supporting Information.

Scheme 4. Schematic Representation of Bond Formation in the TS 5 of Cyclopropanation



One can see that the TS 5 involves the two events (**5a** and **5b**) shown in the bottom of Scheme 4. In **5a**, the nucleophilic attack of the diene terminal to the vacant orbital of the carbene carbon creates a new C–C σ -bond and reduces the metal to the Cu(I) state. In **5b**, the Cu–C(carbene) σ -bond acts as a nucleophile to the allylic cation to close the ring. Here we note two important structural features that influence the stereoselectivity of the cyclopropane formation.

First, the Cu–C_{carbene} σ -bond and the reacting C=C bond need to be parallel to each other to maximize the orbital interactions required in the intramolecular electrophilic cleavage of the Cu–C σ -bond with inversion of stereochemistry. Here, the mutual face selectivity between the Cu=C(carbene) π -bond and the olefinic C=C π -bond must be influenced by two factors: the torsional strain as to the forming bond in **5a** and the steric hindrance between the ester group and the allylic cation moiety. Because of the dimethyl substitution, the former issue is rather unimportant in the DMHD reaction.

The second factor is relevant to the stereochemical effect of the R³ group (the bulkier this group, the better the diastereoselectivity). Since the side chain and the carbonyl oxygen are hydrogen-bonded, the R³ group protrudes to the side where the diene comes in (cf. Scheme 3) and therefore exerts a steric influence on the diastereoselection. In fact, the free energy barrier for the (+)-cis isomer formation was calculated to be 14.0 kcal/mol at the B3LYP/6-31G(d) level, which is 1.1 kcal/mol higher than that for the (+)-trans isomer.³¹ The steric effect between the ester R³ group and the π -allylic moiety in the TS **5** controls the C₁/C₃ relative stereochemistry.

B. Conformation of Copper(I)–Carbene Complex. In the previous section, we found that the interaction between the copper 3d_{xz} and the carbene 2p orbital fixes the orientation of the carbene 2p orbital relative to the salicylidimine moiety, and the intramolecular hydrogen bond between the hydroxyl hydrogen and the carbonyl oxygen transmits the side-chain chirality to the carbene center.

To understand how the chirality in the imine side chain is translated into the stereochemistry in the cyclopropanation product, we first need to study the conformation of the hydrogen-bonded chelate. To this end we studied the conformation of the simplified achiral model **IIa**, where the benzene ring in **I** is

replaced with one double bond. Then we studied the TS of cyclopropanation of **IIb** based on the stable conformers of **IIa**.

Conformations of Achiral Model Complex IIa. The achiral model **IIa** was examined to probe the basic conformational behavior of the carbene complex. Having a double chelate structure (copper chelate and proton bridges), **IIa** has rather limited conformational possibilities: Seven stable conformers (**7–13**) are shown in Figure 4. Among these conformers, **7** is the most stable conformer, where the hydrogen-bond distance is 1.825 Å. Conformer **11** is the highest energy conformer, less stable than **7** by 2.9 kcal/mol in Gibbs free energy or 3.3 kcal/mol in electronic energy. The hydrogen-bond distance of **11** is 2.062 Å, which is significantly longer than that for **7**.

In conformer **12**, hydrogen bonding occurs between the hydroxyl group and the alkoxy oxygen of the ester group. The conformation of the nine-membered ring in **12** is similar to the one found in **7**, but **12** is less stable than **7** by 2.5 kcal/mol in Gibbs free energy or 2.9 kcal/mol in energy because of the less favorable hydrogen bonding. Conformer **13** is the lowest energy conformer among those lacking hydrogen bonding (not shown) and is less stable than **7** by 2.2 kcal/mol in Gibbs free energy or 3.7 kcal/mol in electronic energy.

We conclude from this conformational analysis that the most stable conformation of the copper–carbene complex has a chelate structure in which an intramolecular hydrogen bond is formed between the carbonyl oxygen of the carbene ester group and the hydroxyl hydrogen in the imine side chain.

Conformation of Chiral Model IIb. With the structures of stable conformers **7–13** in hand, we studied the chiral model (**IIb**) bearing R¹ = Me and R² = Ph as a model of the real catalyst, where R¹ is methyl and R² is a substituted phenyl group (Scheme 1). The optimized structures, relative Gibbs free energies at 298 K, and electronic energies are shown in Figure 5. Through introduction of the R¹ and R² groups to **7** and its mirror image (denoted as **7'**) following structure optimization, we generated **20** and **14**, respectively, so that the stereochemistry of the stereogenic center next to the Me (R¹) group becomes an (*R*) configuration. The same procedure was applied to generate **21** and **15** from **8** and **8'**, **17** and **18** from **9** and **9'**, **22** and **15** from **10** and **10'**, and **16** and **19** from **11** and **11'**. It was noted that **8'** and **10'** give the same conformer **15** after optimization.

In these chiral models, there are large differences in energy among the conformers. For instance, the difference between the highest energy conformer **22** and the lowest energy conformer **14** is 9.1 kcal/mol for the Gibbs free energy or 8.5 kcal/mol for the electronic energy. (Note, however, that the most stable conformer **14** was found not to lead to the most favorable TS of cyclopropanation; vide infra.)

These nine structures can be classified into two groups, **14–17** (top row) and **18–22** (bottom row). In the first group, the orientation of the methyl group (R¹) is downward from the plane composed of Cu and the ligand N and O atoms. In addition, the two phenyl groups of R² are oriented upward from the plane, i.e., toward the direction opposite to the methyl group. The orientation of the ester group is also classified into two groups, **14** and **15** versus **16** and **17**.

(31) The Cartesian coordinates of optimized geometry and electronic energy for the TS of (+)-cis-chrysanthemate are described as S-7 in Supporting Information.

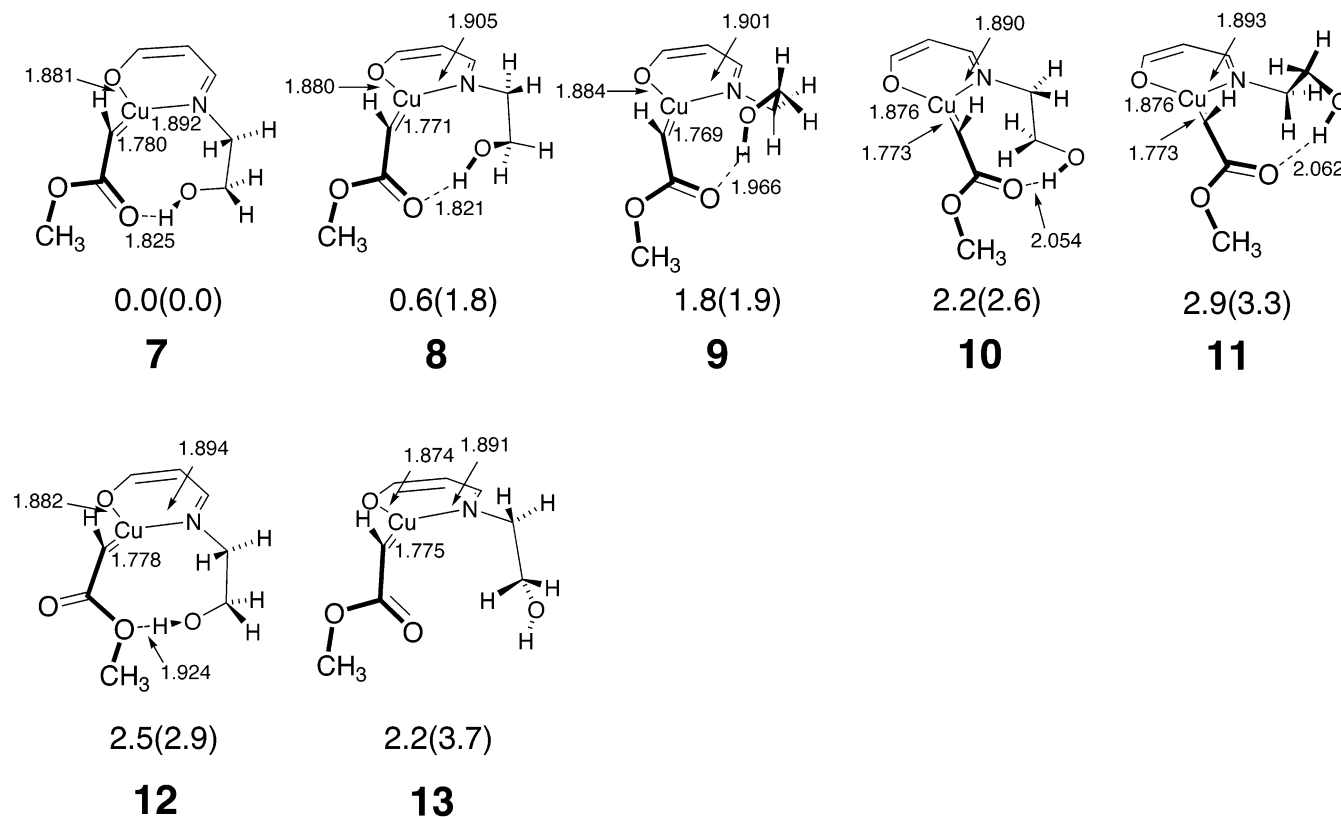


Figure 4. Optimized structures of the copper(I)-carbene complex for the achiral model catalyst **IIa** ($R^1 = H$ and $R^2 = H$) at the B3LYP/6-31G(d) level. Relative Gibbs free energies at 298 K are given in kilocalories per mole (relative electronic energies are shown in parentheses). Numbers next to bonds are bond distances in angstroms.

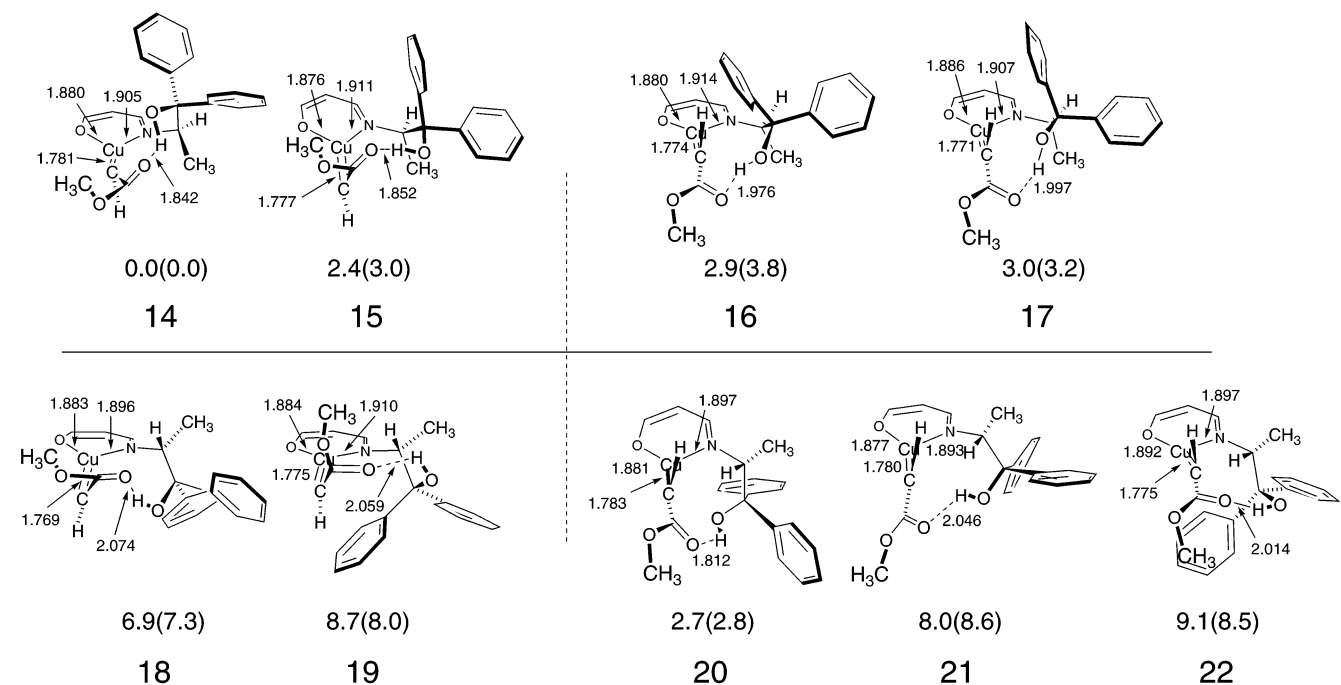


Figure 5. Optimized structures of the copper(I)-carbene complex of the chiral model catalyst **IIb** ($R^1 = Me$ and $R^2 = Ph$) at the B3LYP level of theory. The 3-21G basis set was used for R^1 , R^2 , and the ester methyl group. The 6-31G(d) basis set was used for the remaining atoms. Relative Gibbs free energies at 298 K are given in kilocalories per mole (relative electronic energies are shown in parentheses). Numbers next to bonds are bond distances in angstroms.

In the second group (**18–22**), the orientation of the methyl group (R^1) is upward from the plane and the two phenyl groups (R^2) are downward from the plane, i.e., located in the direction opposite those for the first group. The conformers in the second group except **20** are much higher in energy than those in the

first group. The orientation of the ester group in **18** and **19** is different from the one in **20**, **21**, and **22**.

On the basis of this conformational analysis, one can infer the stereochemistry of the [1 + 2] cycloaddition from each of the nine conformers. The conformers **16**, **17**, **20**, **21**, and **22**

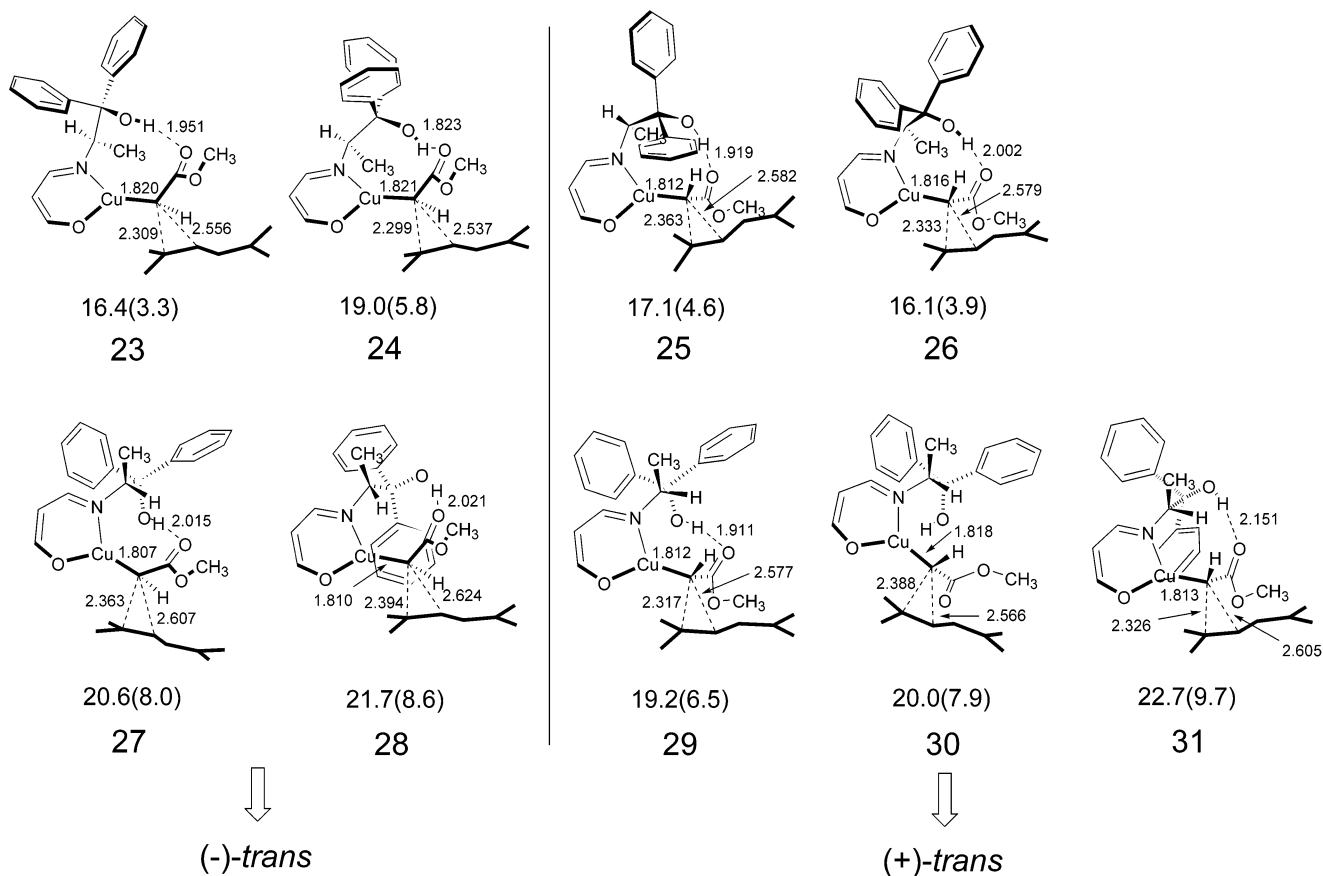


Figure 6. Optimized structures of the transition states corresponding to the formation of the (-)-trans or (+)-trans isomers for the chiral model catalyst **IIb** ($R^1 = \text{Me}$ and $R^2 = \text{Ph}$) with the B3LYP level of theory. The 3-21G basis set was used for R^1 , R^2 , and the ester methyl group. The 6-31G(d) basis set was used for the remaining atoms. Free energies of activation at 298 K are given in kilocalories per mole (activation energies are shown in parentheses). Numbers next to bonds are bond distances in angstroms.

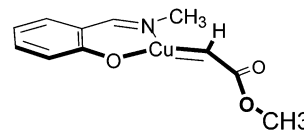
differ from **14**, **15**, **18**, and **19** in the orientation of the ester group.

Since the diene can approach the carbene only from the side opposite the imine side chain (Scheme 3), the chirality of the C^1 center in the cyclopropane product depends on the orientation of the ester in the complex; thus, **16**, **17**, **20**, **21**, and **22** give the (+)-1*R* isomer (which is experimentally observed), while **14**, **15**, **18**, and **19** give the (-)-1*S* product.

C. Transition State of Cyclopropanation. As discussed above, the absolute stereochemistry of the stereogenic center bonded to the ester group (C^1) is determined by the orientation of the ester group with respect to the salicyclaldimine copper chelate, and the C^3 stereochemistry bearing the 2-methylpropenyl side chain is determined by the orientation of the diene relative to the ester group (**5b**, specifically, to avoid the steric effect of R^3). Taking this principle of stereoselection into account, we started with the nine conformers obtained above and allowed them to react with DMHD to give methyl *trans*-chrysanthemate and obtained the nine TSs shown in Figure 6. The TSs grouped on the left-hand side produce the (-)-isomer and those on the right produce the (+)-isomer (the major enantiomer observed experimentally). The correspondence between the copper carbene complexes as starting structures in Figure 5 and the TSs in Figure 6 are **14** and **23**, **15** and **24**, **16** and **25**, **17** and **26**, **18** and **27**, **19** and **28**, **20** and **29**, **21** and **30**, and **22** and **31**. In TS **30** the intramolecular hydrogen bond is broken, while it is kept in the other eight TSs.

In Figure 7, we have summarized the energetics of the cyclopropanation reaction starting with complexes **14**–**22** by way of TSs **23**–**31**. This figure indicates how complex the origin of the Aratani catalysis is indeed. Assuming that the $\text{Cu}-\text{C}_{\text{carbene}}$ bond rotates during the cyclopropanation reaction,³² we can calculate the enantioselectivity of the Aratani cyclopropanation with ligands $R^1 = \text{Me}$ and $R^2 = \text{Ph}$ to be (+):(-) = 66.2:33.8 (Boltzmann distribution at 298 K).³³ The TSs **25** and **26** are the major contributors to the (+)-selective cyclopropanation.

(32) The free energy barriers (298 K) of rotation for the $\text{Cu}-\text{C}_{\text{carbene}}$ bond were calculated for the model below, where the intramolecular hydrogen bonding is neglected. The calculated free energy barriers are 12.3 and 13.2 kcal/mol (two maxima owing to the relative orientation of the side chain and the ester group) by single-point calculations at the B3LYP/6-311+G(d,p) level with the optimized geometries and frequencies at the B3LYP/6-31G(d) level. For comparison, the free energy barriers for the cyclopropanation were also calculated at the same level. For instance, those for **23** and **26** in Figure 6 are 12.9 and 12.1 kcal/mol, respectively. It may be noted that the comparable levels of the two activation energies obtained by the theoretical/chemical model does not rigorously satisfy the Curtin–Hammett conditions that are assumed in the present study.



(33) The enantioselectivity calculated for the energy differences of the TSs at the B3LYP/6-311+G(d, p)//B3LYP/6-31G(d)+3-21G level was (+):(-) = 76.0:24.0 (Boltzmann distribution at 298 K), the same trend as in the text. The one based on the stability of the carbene complexes at the same level was (+):(-) = 28.8:71.2, the trend again the same as in the text and hence contradictory with the experimental data. The original data on these one-point energies are shown in Figure S4 in Supporting Information.

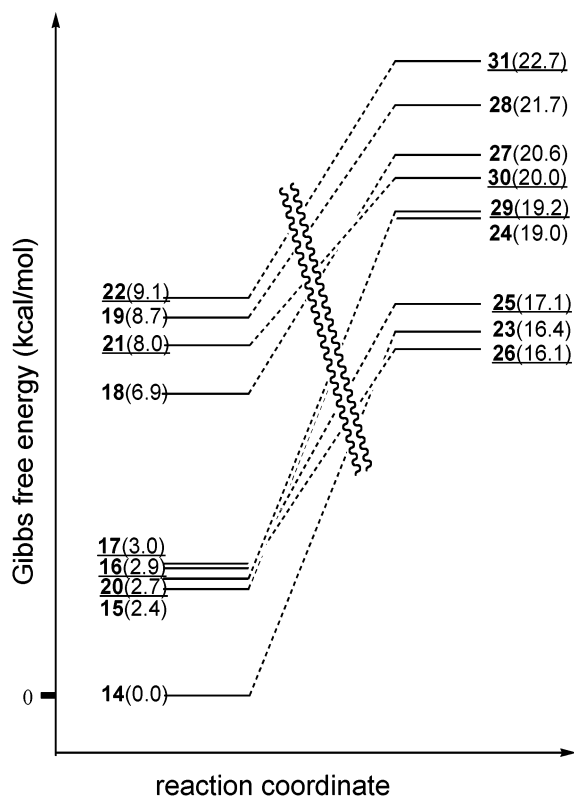


Figure 7. Gibbs energies of the chelate carbene complexes **14–22** reacting with DMHD through TSs **23–31**. The underlined TSs give rise to the (+) enantiomer, while others produce the (–) isomer. See Figure S4 in Supporting Information for the data at B3LYP/6-311+G(d,p)//B3LYP/6-31G(d)+3-21G level that lead to the same conclusion as obtained from this graph (see also footnote 33).

The sense of the selectivity calculated from the TS energies agrees with the experimental selectivity for the particular ligand, that is, 80:20 in favor of the (+) isomer.^{6,34} As seen in the 3D pictures of the major contributors **25** and **26** shown in Figure 8, the Me (R^3) group of the ester moiety occupies the least hindered location and therefore controls the spatial orientation of the diene, which is already quite restricted owing to electronic reasons (Scheme 4). This spatial arrangement is consistent not only with the picture that we described in Schemes 3 and 4 but also with the experimental fact that the stereoselectivity increases as the R^2 phenyl groups bears a bulky ortho substituent such as an octyloxy group and the R^3 ester group becomes a bulkier group such as *tert*-butyl ester.⁶ Note that if we assume that the selectivity solely depend on the relative stability of the carbene conformers **14–22**, the selectivity would be (+):(–) = 2.3:97.7.

We note in passing that the present model (see Figure S2 in Supporting Information) reproduces the reversed selectivity at C^1 (*S* instead of *R*) in the cyclopropanation of 2-methyl-5,5,5-trichloro-2-pentene via the Aratani catalyst^{2,3,6,7} but predicts a near 1:1 mixture of *cis* and *trans* isomers, which is slightly *cis*-rich (5.7:1) in experiments.

IV. Conclusions

As described in the preceding section, the careful analysis of various conformers of the TSs for cyclopropanation resulted in the correct prediction of the enantioselectivity of the Aratani cyclopropanation reaction. Admittedly, the success must be viewed as being fortuitous for several reasons: Even our model

system is too large to study with the most reliable current theoretical method and is too complex for us to explore all conformations and configurations of intermediates and transition states. In addition, the current model calculations do not satisfy the Curtin-Hammett conditions³² as to the rates of Cu=C rotation and the cyclopropanation: This is a difficult problem to solve since there is no detailed experimental (especially kinetic) information on the mechanism of the Cu=C bond rotation or of any other processes to which the calculations should refer. The current level of the quantum mechanical calculations is such that they can generate data that we would never be able to probe by experiments. This may, however, be the reason theory is necessary for experimental chemists who have so far tended to rely on their intuition rather than on theory. In any event, the molecular structures and the analysis described above will provide valuable information on the mechanism of the asymmetric induction by use of the C_1 -asymmetric catalyst.

The Aratani catalyst is C_1 -symmetric and its mechanism of asymmetric induction has been difficult to understand: The mechanism of asymmetric induction reported above is entirely different from the previous speculations (Scheme 2) on which our study was initially based. The selectivity originates from the fact that the alkoxy carbonyl carbene complex is intrinsically chiral as shown in Scheme 3 and that the intramolecular hydrogen bonding transmits the chirality information from the side chain to the carbene complex. This principle of stereoselectivity is different from that in the cyclopropanation by C_2 -chiral ligand¹³ that is controlled largely by the global shape of the chiral environment.³⁵

In this section, we summarize the findings in the following order: (1) molecular orbital basis of the relative orientation of the carbene moiety and the salicylaldimine, (2) fixation of the chiral side chain by intramolecular hydrogen bonding, (3) stereochemical constraint of the cyclopropane formation, and (4) steric effects in the TS of the cyclopropane formation.

(1) The Cu– C_{carbene} σ -bond naturally provides the major force to connect the alkoxy carbonyl carbene group to the copper metal. Much less recognized so far is that the Cu–C σ -bond is conjugated with the carbonyl group (Chart 1a) and hence the orientation of the alkoxy carbonyl group is restricted.^{12,29} Back-donation from the metal to the carbene carbon also restricts the geometry of the complex. The nitrogen–copper–oxygen array assumes a bent geometry (Chart 1b), which raises the energy level of the $3d_{xz}$ group so as to maximize the interaction between the copper $3d_{xz}$ orbital and the carbene vacant 2p orbital. This is similar to the interaction of diorganocuprate with an electron-deficient olefin or with an alkyne (Chart 1c).³⁶ As the result, the geometry around the copper atom is planar and Y-shaped, and the rotation of Cu– C_{carbene} bond is restricted.

(2) These σ - and π -bonding characteristics make the carbene complex chiral and therefore create a diastereomeric relationship between the carbene complex moiety and the stereogenic center in the side chain of the Aratani catalyst. The hydrogen-bonding

(34) Though a low ee value [favoring the (+) isomer] was reported for this ligand ($R^1 = \text{Me}$ and $R^2 = \text{Ph}$) in the original Aratani paper (ref 6), a recent experiment under better controlled conditions showed an enantioselectivity of 60% ee (ref 17d). It should be noted that ethyl diazoacetate (i.e., $R^3 = \text{Et}$) was used in these experiments, whereas R^3 is a methyl group in this study.

(35) Nakamura, M.; Arai, M.; Nakamura, E. *J. Am. Chem. Soc.* **1995**, *117*, 1179–1180.

(36) Nakamura, E.; Mori, S. *Angew. Chem., Int. Ed.* **2000**, *39*, 3750–3771.

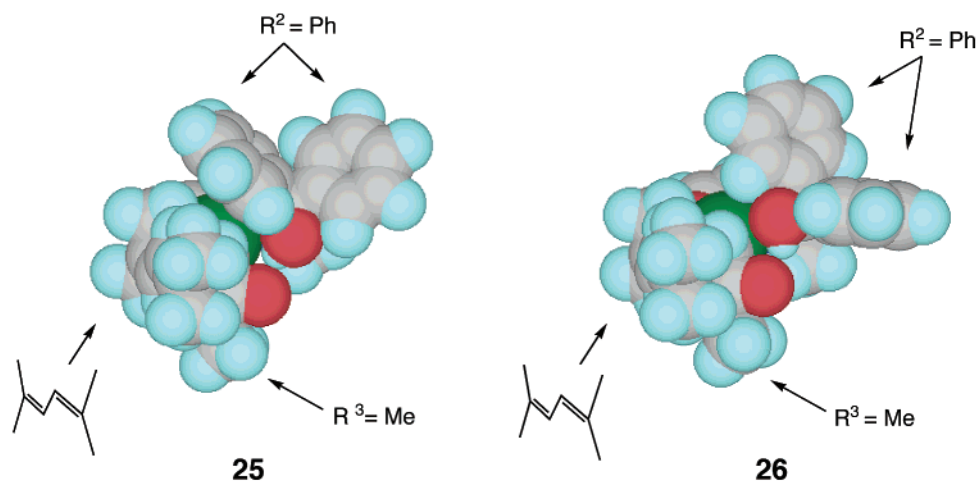
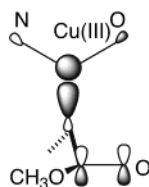


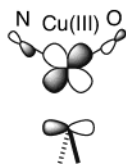
Figure 8. Three-dimensional structures of TSs **25** and **26** that illustrates the effect of the R^2 groups to steer the orientation of the COOMe (i.e., COOR³) group and hence that of the diene. The atoms are depicted as follows: C, gray; Cu, green; H, blue; O, red.

Chart 1. Molecular Orbital Interactions in Copper–Carbene Complexes (a, b) and in a Cuprate/Acetylene Complex (c)^a

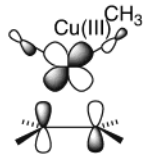
(a) Donation and σ -metal-ester character



(b) Back-donation

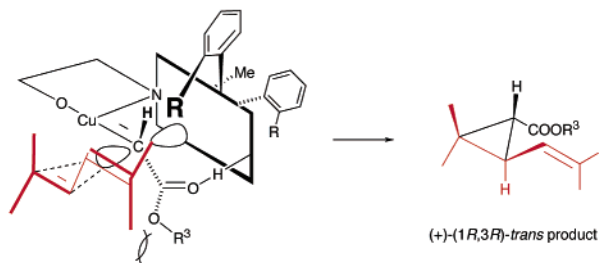


(c) Back-donation in Me₂Cu⁺/olefin



^a The copper atom is described in its trivalent state as the result of back-donation to the carbene vacant 2p orbital (a) and to the olefin π^* orbital (c).

Scheme 5. Schematic Drawing of the Relative Stereochemistry in the TS of the Aratani Cyclopropanation



between the OH group and the ester carbonyl orients the ester alkoxy group (OR³) to protrude in the direction from which the olefin (DMHD) comes in (Scheme 5).

(3) The cyclopropanation involves two events that are taking place simultaneously, which defines the relative orientation of the Cu–C and the developing allylic cation center in the TS (Scheme 4). One of the two R^2 phenyl groups bears a bulky ortho R group in the experiment (Scheme 5), and the R group exerts a steric influence over the orientation of the R^3 group.

(4) With these electronic and steric steering effects, the Me₂C=C group of DMHD seeks a sterically most favorable position by avoiding interaction with the R and R^3 groups and produces the (+)-*trans*-chrysanthemic ester.

In summary, we have described the reaction mechanism of the synthesis of chrysanthemic acid methyl ester in the presence of a salicylaldehyde Cu(I) complex and provided a reasoning for the mechanism of asymmetric induction on the basis of electronic properties of the carbene complex and the TS of cyclopropane formation. The present theoretical study has been instrumental in the development of an industrial process for chrysanthemic acid at Sumitomo Chemical Co. and will be useful also for those engaged in the use of the salicylaldehyde ligand in organic synthesis.³⁷

Acknowledgment. We thank Drs. Aratani and Suzukamo for their helpful advice and discussion and Drs. Yanagi and Hassila for providing us their doctoral thesis related to our work. The calculations were performed by use of computational facilities at Tsukuba Research Laboratory and Organic Synthesis Research Laboratory in Sumitomo Chemical Co., Ltd. The research at the University of Tokyo was supported by Monbukagakusho (Grant-in-Aid for Special Research, and the 21st Century Center of Excellence project).

Supporting Information Available: Cartesian coordinates and electronic energies of the stationary points (PDF). This material is available free of charge via the Internet at <http://pubs.acs.org>.

JA031524C

(37) (a) Su, J. T.; Vachal, P.; Jacobsen, E. N. *Adv. Synth. Catal.* **2001**, *343*, 197–200. (b) Li, Z.; Chen, H. *React. Kinet. Catal. Lett.* **2001**, *73*, 217–222. (c) Shi, M.; Wang, C.; Chan, A. S. C. *Tetrahedron: Asymmetry* **2001**, *12*, 3105–3111. (d) Katsuki, T. *Synlett* **2003**, 281–297.